9

Research article

Chuantong Cheng^a, Beiju Huang^{a,*}, Xurui Mao, Zanyun Zhang, Zan Zhang, Zhaoxin Geng, Ping Xue and Hongda Chen

Monolithic optoelectronic integrated broadband optical receiver with graphene photodetectors

https://doi.org/10.1515/nanoph-2017-0023 Received February 6, 2017; revised March 29, 2017; accepted April 11, 2017

Abstract: Optical receivers with potentially high operation bandwidth and low cost have received considerable interest due to rapidly growing data traffic and potential Tb/s optical interconnect requirements. Experimental realization of 65 GHz optical signal detection and 262 GHz intrinsic operation speed reveals the significance role of graphene photodetectors (PDs) in optical interconnect domains. In this work, a novel complementary

metal oxide semiconductor post-backend process has been developed for integrating graphene PDs onto silicon integrated circuit chips. A prototype monolithic optoelectronic integrated optical receiver has been successfully demonstrated for the first time. Moreover, this is a firstly reported broadband optical receiver benefiting from natural broadband light absorption features of graphene material. This work is a perfect exhibition of the concept of monolithic optoelectronic integration and will pave way to monolithically integrated graphene optoelectronic devices with silicon ICs for three-dimensional optoelectronic integrated circuit chips.

Keywords: graphene photodetectors (GPDs); optoelectronic integration; optical receiver.

Chuantong Cheng and Beiju Huang: These authors contributed equally to this work.

*Corresponding author: Beiju Huang, State Key Laboratory of Integrated Optoelectronics, Institute of Semiconductor, Chinese Academy of Sciences, Beijing 100083, China; and College of Materials Science and Opto-Electronic Technology, University of Chinese Academy of Sciences, Beijing 100049, China, e-mail: bjhuang@semi.ac.cn

Chuantong Cheng: State Key Laboratory of Integrated Optoelectronics, Institute of Semiconductor, Chinese Academy of Sciences, Beijing 100083, China; State Key Laboratory of Low-Dimensional Quantum Physics and Center for Atomic and Molecular Nanoscience, Department of Physics, Tsinghua University, Beijing 100084, China; and College of Materials Science and Opto-Electronic Technology, University of Chinese Academy of Sciences, Beijing 100049, China Xurui Mao and Hongda Chen: State Key Laboratory of Integrated Optoelectronics, Institute of Semiconductor, Chinese Academy of Sciences, Beijing 100083, China; and College of Materials Science and Opto-Electronic Technology, University of Chinese Academy of Sciences, Beijing 100049, China

Zanyun Zhang: School of Electronics and Information Engineering, Tianjin Polytechnic University, Tianjin 300387, China

Zan Zhang: School of Electronic and Control Engineering, Chang'an University, Xi'an 710064, China

Zhaoxin Geng: State Key Laboratory of Integrated Optoelectronics, Institute of Semiconductor, Chinese Academy of Sciences, Beijing 100083. China

Ping Xue: State Key Laboratory of Low-Dimensional Quantum Physics and Center for Atomic and Molecular Nanoscience, Department of Physics, Tsinghua University, Beijing 100084, China; and Collaborative Innovation Center of Quantum Matter, Beijing 100084, China

1 Introduction

In this information age, superiority of optical communications becomes obviously evident due to its large bandwidth, low attenuation, high electromagnetic interference immunity, and high reliability. As critical components of optical interconnect systems, optical receivers consisted of photodetectors (PDs) and photocurrent signal amplifier circuits have attracted intensive attention due to huge demand in the market. PD, a device converting transmission optical signals into electrical signals for the following processing, is a core part of an optical receiver. Normally, photocurrent produced by PD is very small due to relatively weak optical signals. Hence, a photocurrent signal amplifier circuit is required in the optical receiver to amplify detected signals. Recently, development of optical receivers with low cost and high performance is a research hotspot [1, 2]. Fortunately, amplifier circuits can be achieved via integrated circuits (ICs) with the complementary metal oxide semiconductor (CMOS) technology and cost will be significantly reduced with the mature microelectronic technology. Therefore, the realization of a costless PD and a cost-effective fabrication process to integrate PDs with IC chips is the urgent problem that remains.

Nowadays, extensive attention have been given to the integration of CMOS compatible PDs and amplifier circuits on a single chip (monolithic optoelectronic integrated circuits, OEICs) for affordable high-performance optical receivers [3-5]. Silicon PD-based optical receivers can be obtained easily with a CMOS compatible technology and are widely used in short-distance optical communications with 850 nm wavelength [6]. However, due to the relatively large bandgap of silicon material, this kind of optical receiver could not detect valuable optical carriers with wavelengths of 1310 and 1550 nm, which are widely used in modern optical communication systems. Nevertheless, germanium (Ge) material with a narrow band gap can detect these light waves [7, 8]. In the front-end of line Si CMOS process design, electronic transistors, and photonic devices are achieved simultaneously [9]. However, to achieve a high-performance Ge PD is very difficult due to allowable limited layer thickness of the Ge material in the standard CMOS process. Moreover, much bigger footprints of PDs occupy valuable transistor real estate leading to higher product cost. Meanwhile, researchers attempted to integrate the Ge crystals on the surface of amorphous silicon with the back-end of line process [10], which can achieve 3D dense integration of photonics and electronics [11, 12]. However, a 3D monolithic optoelectronic integrated optical receiver with Ge PDs has not yet been demonstrated based on this approach. Therefore, a material with potentially high carrier mobility and wide-band photoresponse features is aspired for a monolithic optoelectronic integrated optical receiver. It could be utilized to serve for both short wavelength and long wavelength optical communication systems with a high operation speed. However, this broadband optical receiver has not been reported, to the best of our knowledge.

Graphene, a single sheet of carbon atoms in a hexagonal lattice, is the first two-dimensional (2D) atomic crystal available in the world [13]. Its linear dispersion relation between energy and crystal momentum results in remarkable material parameters and makes it a star contender for lots of applications, especially for electronic [14-17], photonic [18, 19], and optoelectronic applications [20-24]. With zero bandgap, graphene can absorb electromagnetic radiation ranging from far-infrared to UV light [25]. Graphene can fast respond to incident illumination [26-28] due to the ultrahigh carrier mobility (about 200,000 cm 2 V $^{-1}$ s $^{-1}$ in experiment [29]). Therefore, graphene has been considered as an outstanding material for PDs. Although the firstly demonstrated graphene photodetector (GPD) achieves a bandwidth of about 40 GHz [21], the ultrahigh intrinsic operation speeds could be well over 500 GHz [21], surpassing the state-of-the-art PDs [30].

As GPDs can respond to optical signals with a wavelength covering all optical communication bands, the GPD-based optical receivers have a chance to serve both short wavelength and long wavelength optical communications [31]. Meanwhile, graphene material with high quality and large area can be obtained with the low-cost chemical vapor deposition (CVD) technology [32]. Therefore, GPD is the most potential candidate for the realization of a broadband, high speed and cost-effective optical receiver.

Goossens [33] firstly presented a high-resolution image sensor by integrating graphene phototransistors with CMOS ICs. However, a CMOS-compatible GPD-based monolithic optoelectronic broadband optical receiver with high reliability, small size, and low cost is not currently available. In order to fill this gap, we develop a kind of CMOS post-backend process to realize GPDs on the surface of the IC chips and ultimately achieve a monolithic optoelectronic integrated broadband optical receiver. Silicon is perfect to fabricate IC chips for signal amplification and processing benefit from the mature CMOS technology and the graphene material is obviously suitable for optical detection due to its high operation bandwidth and broadband photoresponse. Hence, GPD-based optical receivers take advantage of both silicon material and graphene material simultaneously. Therefore, this scheme shows great potential to realize an optical receiver with low cost and high performance in the near future. Here, prototype of GPD-based broadband optical receiver has been experimentally demonstrated for the first time. GPDs were fabricated on the surface of the silicon nitride passivation layer of the commercial 0.35 µm feature size silicon ICs with a low-temperature CMOS compatible process. Detection sensitivity of GPD on silicon ICs was significantly improved by integrating GPD with the photocurrent amplifier on the silicon chip, which is meaningful when considering limited intrinsic photoresponsivity of GPD due to weak optical absorption of graphene. In consideration of the easily available materials and the excellent combination, this broadband optical receiver of low cost and high performance might find its extensive application in optical communications in the near future. This work not only indicates the realization of a successful broadband optical receiver but also provides a feasible process for monolithic integration of graphene optoelectronic devices and silicon ICs.

2 Device design and fabrication

As massless Dirac fermion, carriers in graphene can move with a speed up to 1/300 light velocity [34], which results in the ultrahigh room-temperature carrier mobility and the achievement of high-speed GPDs. With zero bandgap, graphene can respond to light wave with wavelength covering all optical communication bands (such as 850, 1310, and 1550 nm), which explains GPD's natural broadband character [25]. However, the uniform 2.3% optical absorption of graphene limits GPD's photoresponsivity [35]. To solve this problem, graphene has been integrated with microcavities [36], plasmon resonators [37, 38] and silicon waveguide [23, 24, 39-41], but these methods weaken the broadband character. Another method carried out by integrating graphene layer with semiconductor quantum dots can greatly improve photoresponsivity without wavelength dependence [42], but the photoresponse speed is relatively low.

The aforementioned approaches are all focused on the enhancement of the intrinsic photoresponsivity of GPDs. However, we can amplify weak photocurrent signals from GPD with a simple metal-graphene-metal structure by utilizing an additional current amplifier circuit and this module can be defined as a prototype optical receiver. This optical receiver may exhibit high operation speed, broad spectral bandwidth, and low detection limit simultaneously. Transimpedance amplifiers (TIAs) transforming weak photocurrent into large output voltage are often used in the optical receivers. Here, the innovation is that we integrated GPDs on the surface of the TIA chips for optical receivers of low cost. As a single atom layer material, graphene is fond of a smooth substrate. A rough surface would result in sidesteps in the graphene layer,

which would cause serious degradation of the performance of grapheme-based devices. Hence a commercial 0.35 µm feature size silicon CMOS technology is adopted to achieve TIAs as the surface of the chip away from the pads is smooth.

Figure 1A shows three-dimensional (3D) schematic of GPD-based broadband prototype optical receivers. The GPD with a simple metal-graphene-metal structure is fabricated on the smooth surface of the silicon-based IC chips. An inductance L and a capacitance C from a high-performance bias-tee are utilized to apply DC bias for GPD and extract output photocurrent for TIA input (TIA_{in}), respectively. Figure 1B shows the corresponding circuit implementation of the prototype optical receivers. Output photocurrents from GPDs are injected into TIAs and amplified voltage signals can be obtained at the TIA output (TIA out).

We began with the design of schematic of TIA ICs and the drawing of the layout, and then the layout data were sent to a CMOS manufacturing foundry line. The 2.5×2.5 mm² IC chips were obtained by wafer dicing. In the following fabrication process, the biggest challenge was to fabricate GPDs on the surface of the silicon nitride passivation layer of the small-sized IC chips. The main fabrication processes of GPDs on the surface of the IC chips are schematically shown in Figure 2. Firstly, the CVD grown graphene film was transferred onto the surface of the 2.5×2.5 mm² IC chip after the copper foil was etched away (Figure 2A). Secondly, the photolithography and O₂ plasma etching were successively used

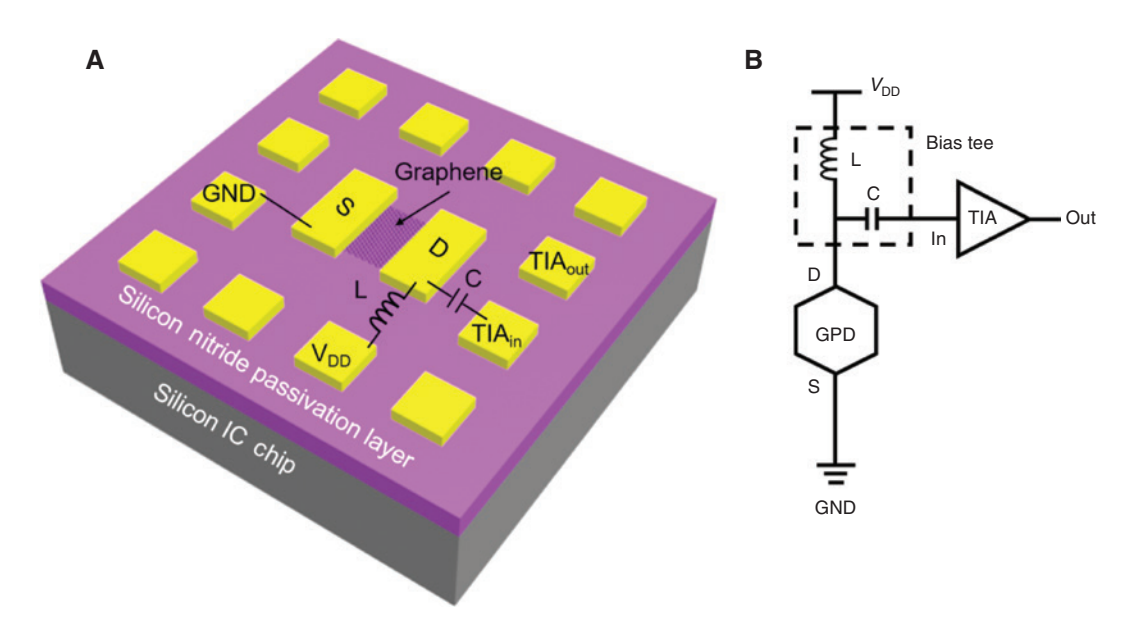


Figure 1: Three-dimensional schematic of GPD-based broadband prototype optical receivers (A) and schematic illustration of the corresponding circuit implementation (B) are shown.

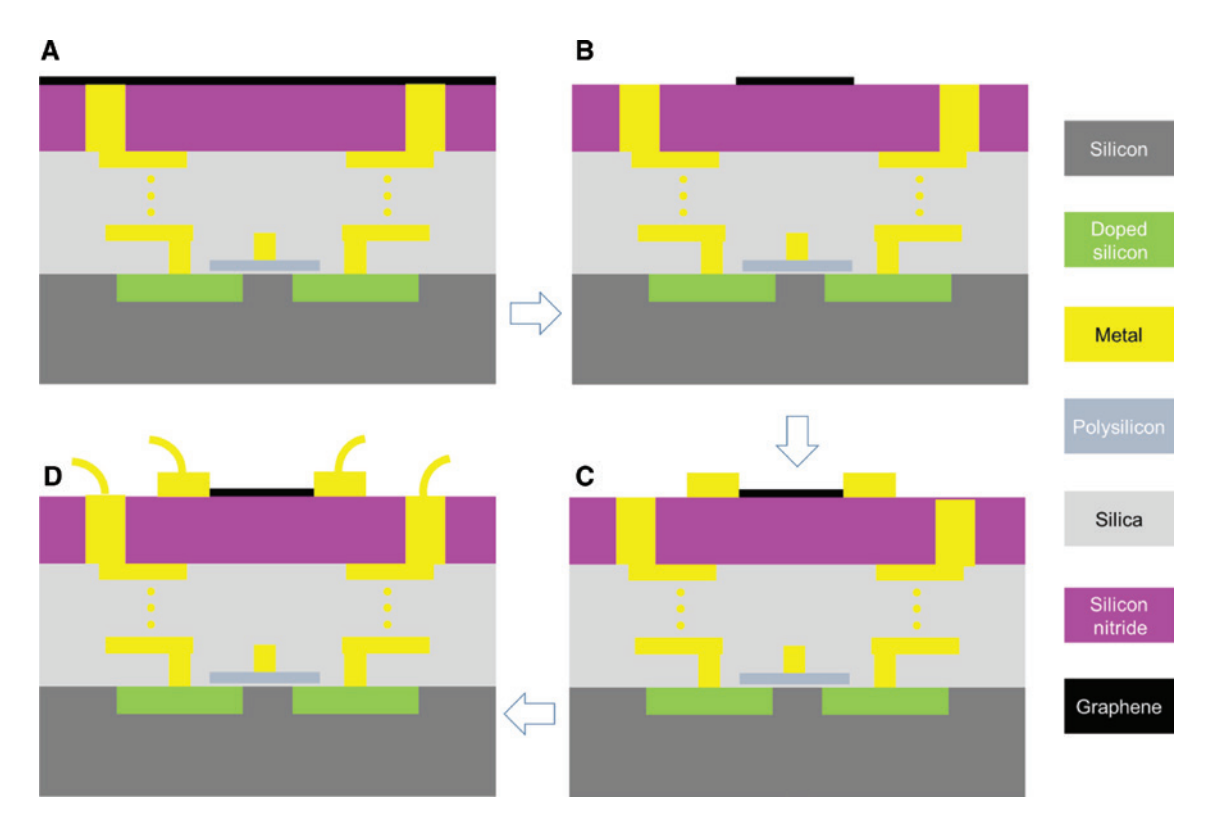


Figure 2: Schematic of main fabrication steps of the optical receiver.

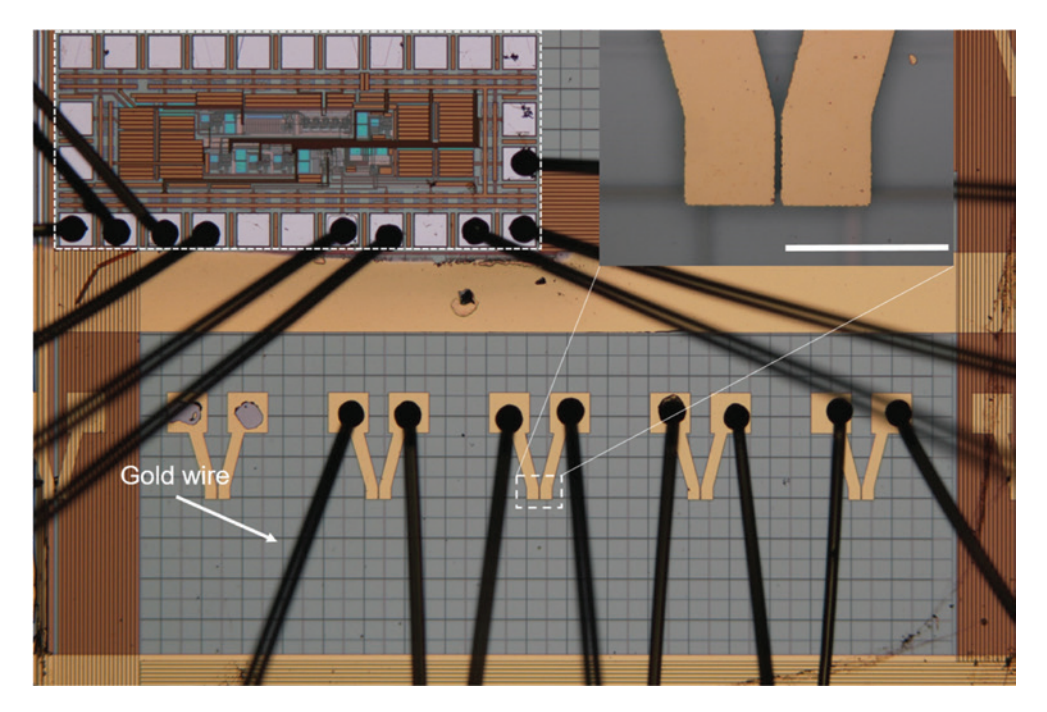
(A) CVD graphene is transferred on the surface of the IC chips. (B) A patterned graphene channel is obtained. (C) Metal contacts of graphene are completed. (D) A wire bonding process is completed for test.

to obtain the patterned graphene channel (Figure 2B). Thirdly, the Ti (10 nm)/Au (150 nm) films working as metal contacts were finished by lift-off in acetone after the photolithography and thermal evaporated processes (Figure 2C). Finally, pads of GPDs and silicon IC chips were wire-bonded to a universal printed circuit board (PCB) (Figure 2D). Here we should give the details about the photolithography process as the size of the IC chip is too small with the normal methods. At first, a silicon chip with size of 15×15 mm² was chosen as the support substrate of the IC chip. Then a thick adhere layer with flat surface was achieved on the surface of the silicon chip via spin coating process with a speed of 1000 rpm for 60 s and the IC chip was placed on the surface of the adhere layer at one of the corners. Then heating for 10 min under 80°C on the planet was carried out to fix the IC chip on the silicon chip firmly for the following regular photolithography process. As the temperatures of all the fabrication processes are lower than 200°C, the performance of the CMOS IC chips would not degenerate. Hence, a feasible CMOS post-backend process has been developed for the realization of monolithic integration of graphene optoelectronic devices and silicon ICs in this work.

3 Results and discussion

3.1 Device characterization

Figure 3 shows optical micrograph of the fabricated GPD-based broadband optical receivers. Five GPDs were achieved on the surface of the IC chip, which means a GPD array can be obtained easily. The thickness of the metal electrodes is only 160 nm (Ti/Au 10 nm/150 nm) in this work, which is a little thin for the wire-bonding process. However, four GPDs were wire-bonded to a universal PCB successfully, which means the Ti adhesion layer could work well on the surface of the silicon nitride layer. A better result might be obtained with thicker metal contact. Here, wire-bonding scheme is carried out for the purpose of the realization of the independent tests of the discrete GPDs and the integrated optical receiver. As performances of GPDs can vary with bias, we should apply different biases to GPDs for the best operation point. These bonding wires can be replaced easily by the metal interconnects with the mature CMOS process. The white dotted frame displays location of TIA IC and the inset at the right top shows GPD with more details. The scale bar is 50 µm. The graphene is



Fgure 3: Optical micrograph of the fabricated GPD-based monolithic optoelectronic integrated broadband optical receivers. The inset shows the GPD with more details and the scale bar is $50 \, \mu m$. The white dotted frame shows the location of the TIA IC.

invisible on the surface of the silicon nitride layer due to low reflection contrast.

Raman spectra measurements were performed to characterize density of defects of the transferred CVD graphene on the surface of the silicon ICs with silicon nitride passivation layer. At the same time, we transferred the CVD graphene onto the surface of the silicon wafers with 300 nm thermal oxide layer for a comparison. The Raman spectra were obtained with a 532 nm excited laser with an incident power of 5 mW and laser spot diameter of 20 µm. As shown in Figure 4A,B, almost no obvious defects were observed in the graphene on the surface of the silica (rea line) and silicon nitride (black line), which means the high quality of the transferred graphene and the smooth silicon nitride layer has no damage to graphene [43]. It should be noted that Raman spectrum of the graphene on the surface of the IC chips was obtained by subtracting the substrate signal from the total signal. Figure 4C,D show the scanning electron microscopy (SEM) image and the atomic force microscopy (AFM) images of the GPD, respectively. The boundary of the graphene layer can be discovered easily in the SEM image because of the high electrical conductivity of graphene. The AFM image shows roughness of 1.6 nm on graphene and 1.8 nm on silicon nitride, which indicates excellent mechanical features of graphene material. Smooth surface is necessary for the achievement of high performance GPDs. As thickness of the single layer graphene is only about 0.4 nm, an

inconspicuous color change can be found at the boundary of graphene.

3.2 Static photoresponse measurement

Before being connected to Si CMOS ICs, the static photoelectric characteristics of GPDs fabricated on the surface of the IC chip were investigated. Figure 5A shows the schematic measurement circuitry. Currents in the circuit under different illumination conditions were measured using a Keithley 2612B semiconductor analyzer. In GPD, a shorter channel length means a higher operation bandwidth. In our fabricated GPD, the channel length is about 3 um. However, a single mode fiber was utilized to guide optical power to the surface of GPDs and the light spot diameter is normally bigger than 11 µm for 1550 nm wavelength. Therefore, less than 25% of the total incident optical power can interact with graphene in GPD channel. A lensed fiber with small spot-size can be utilized to reduce the loss of incoming light in the future. The photocurrents of the GPD versus bias voltages for different effective input optical powers (5, 10, 20 mW) at 1550 nm were shown in Figure 5B. An approximately linear relationship between photocurrents and sweeping bias voltages (from -1 V to 1 V) can be described for fixed input optical power. Same polarity of photocurrent and bias voltage indicates that photovoltaic effect makes a significant contribution to

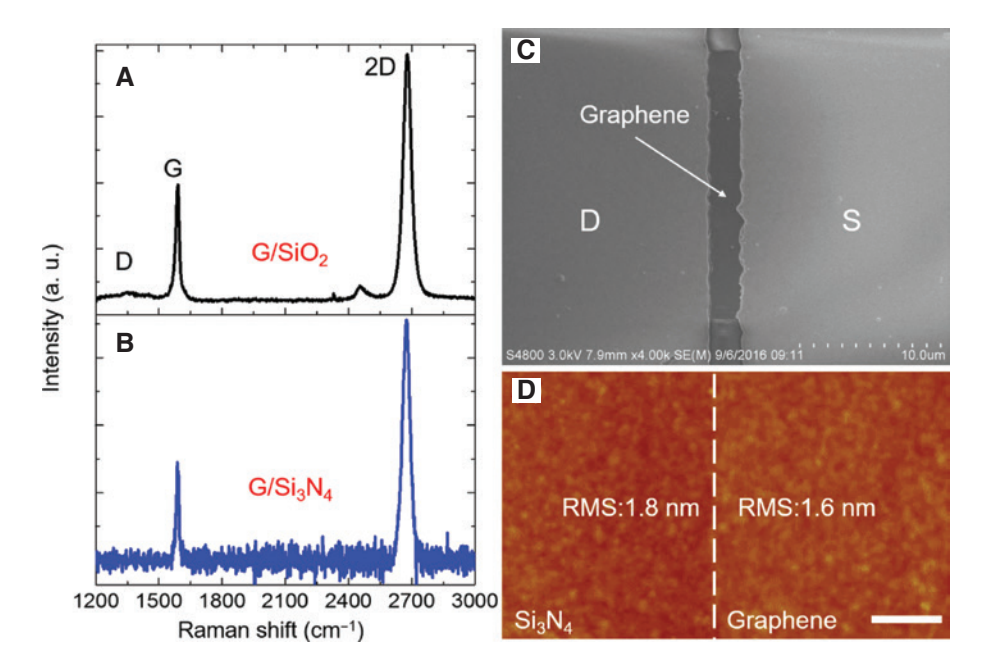


Figure 4: Raman spectra of the transferred graphene on the surface of silica (A) and silicon nitride (B) indicate that the surface of the passivation layer on the IC chip did not bring any additional damages to the performance of the graphene. (C) The scanning electron microscopy image shows the graphene channel clearly due to high electrical conductivity of the graphene material. (D) The atomic force microscopy image at the boundary of graphene and silicon nitride shows more details of the graphene material and silicon nitride. The scale bar is 500 nm.

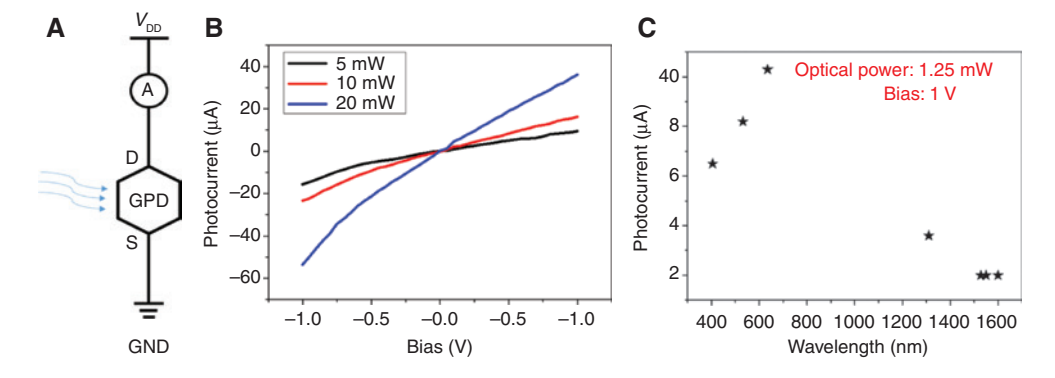


Figure 5: Static photoresponse of optical receivers. (A) Schematic measurement circuitry for static photoresponse features of GPDs. (B) Photocurrents of GPD versus bias voltages for different input optical powers at 1550 nm were shown. (C) Broadband photoresponse of GPD was investigated by using light sources with different wavelengths.

the high responsivity as the external electrical field could accelerate the photon-generated carriers. At a fixed bias voltage, photocurrent increases with input optical powers due to growing number of photon-generated electron-hole pairs.

Broadband photoresponse of GPDs at a bias of 1 V was investigated and the tested photocurrents of 1.25 mW effective incident optical power with different wavelengths (405, 532, 635, 1310, 1528, 1550, and 1600 nm) were shown in Figure 5C. The responsivity of the GPD is about 1.6 mA/W for the illumination with a

wavelength of 1550 nm. For short wavelengths, a higher responsivity about 8 mA/W is obtained probably due to hot-carrier effect [44]. This photoresponsivity is comparable with the reported pure graphene-based PD on silica substrate [21], which indicates an excellent compatibility of graphene material and silicon nitride passivation layer. Here, we should note that this is the first time that GPD was fabricated on the surface of a standard silicon IC chip successfully. Benefiting from broadband photoresponse of GPD on surface of the TIA IC chips, a costeffective monolithic optoelectronic integrated optical receiver with broadband photoresponse was achieved for the first time.

3.3 Dynamic performance measurement

The dynamic responses of GPDs and the optical receivers were measured using a test circuitry as shown in Figure 6A. A 1550 nm continuous-wave from the laser diode was modulated with a Mach-Zehnder modulator driven by a signal generator (Agilent 33250A) and a 500 kHz optical sinusoidal signal was generated. Before the optical signals were focused onto GPDs, an erbiumdoped fiber amplifier was used to amplify optical signal power. A high-performance bias tee was used to apply DC bias to GPDs and extract the output photocurrent signals. In order to investigate the current amplification features of TIA, two output modes were carried out. In mode 1, the output signals were observed by an oscilloscope (Agilent MSO-X3034A) directly. In mode 2, the output photocurrent signals were amplified by TIAs firstly. Figure 6B shows output voltages of the photocurrent signals at 1 V bias with (red) and without (black) TIAs under 20 mW effective incident optical power. The $V_{\rm nn}$ (peak to peak voltage) of the black waveform is 13 mV while the V_{nn} of the red waveform is 291 mV, which means 22-fold photocurrent signal enhancement is achieved at bias of 1 V successfully. Figure 6C displays the output V_{nn}

with (red) and without (black) TIAs as a function of the bias under 20 mW effective optical power. At zero bias, output V_{pp} without TIAs is small than 0.01 mV, however, the output V_{pp} with TIAs is about 35 mV, which indicates the realization of a more than 3500 times signal amplification. As the magnification times increase obviously with the decrease of the bias, this optical receiver can operate with very low power consumption. In order to investigate the performances of the GPD-based optical receiver under a relative small effective incident optical power, the output voltages of the optical receiver at 1 V bias under a 2 mW effective incident optical power was obtained and shown in Figure 6D. The V_{pp} of the output voltage is more than 50 mV, which means a much smaller optical power can be detected with this OEICbased optical receiver.

As dark current of fabricated GPD is 325 µA at 1 V bias, power consumption is 325 µW. The relatively large power consumption results from zero bandgap of graphene material. The GPD with asymmetric metal contacts [22] operated at zero bias can be fabricated on the surface of IC chips for zero power consumption of optical receivers in the near future. Total capacitance of a GPD consists of pad capacitance (C_n) and graphene capacitance (C_n) . C_n is related to the structure of pads in GPD and C_g is related to both total channel charge and channel graphene area. In principle, small pads and small graphene area mean low device capacitance. With results in Ref. [21], total

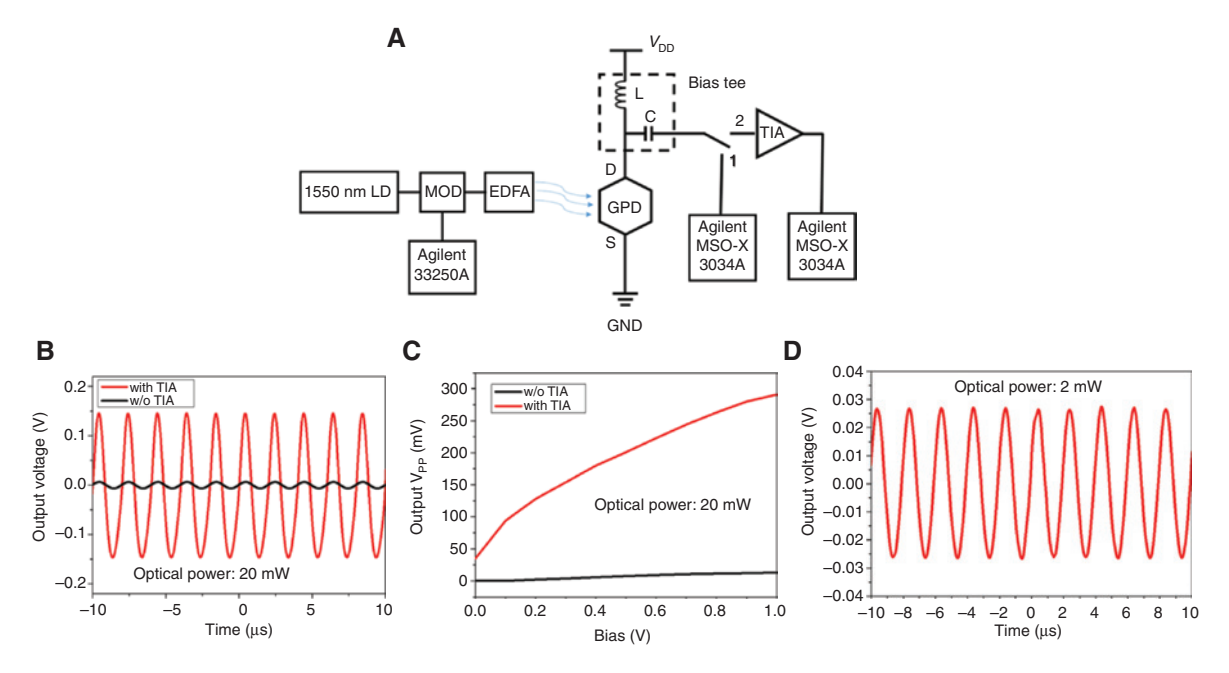
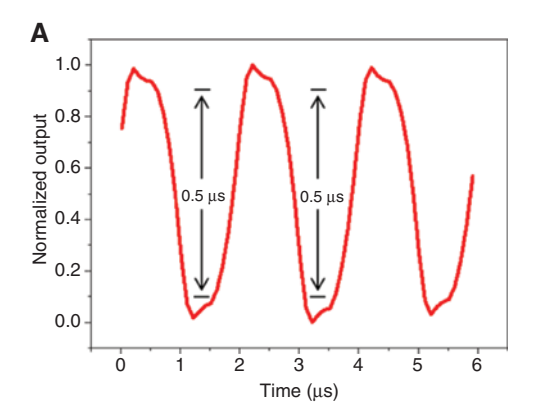


Figure 6: Dynamic photoresponse of optical receivers.

(A) Test circuitry for dynamic responses of GPD and the optical receiver. (B) Output voltages of the photocurrent signals at 1 V bias in mode 1 (black) and mode 2 (red). (C) Output V_{pp} values of mode 1 (black) and mode 2 (red) as a function of the bias. (D) Output voltages of the optical receiver at 1 V bias under a 2 mW effective optical power with a frequency of 500 kHz.



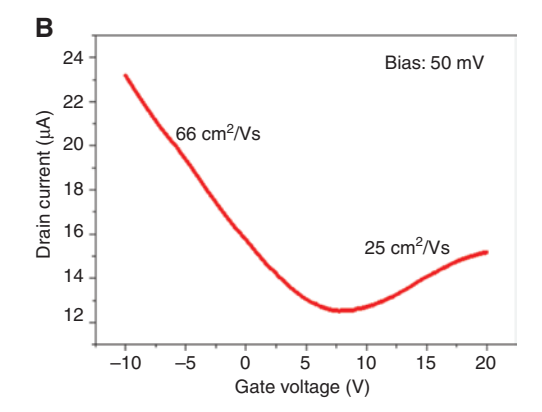


Figure 7: Photoresponse rate of the used CVD graphene material.
(A) Normalized output signals of GPDs for pulsed optical signals. (B) Transfer curve of GFETs fabricated with same graphene as GPDs and carrier mobility of the graphene material.

capacitance of our fabricated GPD is less than 230 fF, where $C_{\rm p}$ (pad structure: $100\times100~\mu{\rm m}^2$ in size and 50 $\mu{\rm m}$ in distance) is less than 30 fF and $C_{\rm g}$ (graphene area: $3\times20~\mu{\rm m}^2$) is less than 200 fF. Therefore, a small graphene area in GPD is required for a small capacitance and thus high bandwidth in the future.

Figure 7A shows the normalized output signals of GPDs for the pulsed optical signals. Rise time and fall time are 0.5 and 0.5 μ s, respectively, which means the bandwidth of fabricated GPD is 700 kHz. The relative low bandwidth is attributed to the relative low carrier mobility of the commercial CVD graphene utilized in GPDs. Carrier mobility of the CVD graphene used in the GPDs in our work can be obtained from the transfer curve of graphene field effect transistors (GFETs). We have fabricated a GFET with the same graphene material and fabrication process as the GPDs. The transfer curve under 50 mV bias is displayed in Figure 7B. The carrier mobility for holes (electrons) is 66 cm² V⁻¹ s⁻¹ (25 cm² V⁻¹ s⁻¹), which is much smaller than the single crystal graphene obtained via a mechanical exfoliated process [29].

3.4 Discussion

Finally, we discuss the potential superiorities of the GPD-based monolithic optoelectronic integrated optical receiver for future optical communication applications.

(1) **Broadband optical receiver.** With zero band gap, graphene material can absorb electromagnetic radiation in ultra-wide wavelength range. In this work, GPDs can operate from 405 to 1600 nm, which covers the most important three optical communication wavelengths (850, 1310, and 1550 nm). Therefore, this GPD-based broadband optical receiver can serve almost all optical communication systems.

- (2) Potentially high operation bandwidth. As potential carrier mobility of graphene is extremely high, the operation bandwidth of GPD is limited by RC constant of the device structure and a 500 GHz [21] intrinsic operation speed can be achieved in the future. Although the first graphene-based optical receiver achieved in this work just works at 500 kHz with 1550 nm carrier waves, the performance can be improved significantly if a single crystal graphene with higher carrier mobility is used and an optimized fabrication process [45] is carried out to reduce contact resistance and remove residue on the graphene surface. In addition, further collaborative parameter optimization of the TIA chips and GPDs may increase the operation speed to a great extent. Hence, a lot of work can be developed to improve the performances of GPDs in the future.
 - Monolithic optoelectronic integration. OEICs are kind of novel devices that integrate optoelectronic components and electronic ones on one chip and have attracted strong interest for their advantages of small size and high reliability, and will find its roles in many applications related to photonic and optoelectronic domains. Here, a CMOS backend process compatible scheme has been provided to integrate GPDs with simple MGM structure onto the standard IC chips for a monolithic OEIC-based optical receiver. Actually, this integration scheme can support the monolithic integration of optical waveguide-based GPDs and silicon IC chips. Silicon nitride material can work as an optical guiding medium due to its good optical characteristics and CMOS compatible features. Integrating graphene with silicon nitride waveguide is a potential scheme to achieve GPD with high responsibility and broadband photoresponse. In our former works, we have monolithically integrated silicon

nitride waveguides with IC chips through a postbackend process successfully [12]. Hence, a silicon nitride waveguide integrated GPD and even a waveguide integrated graphene optical modulator can be achieved facilely along the waveguides. Therefore, with silicon nitride material and graphene, both passive photonics devices and active optoelectronic ones can be monolithically integrated with IC chips and 3D OEIC with high integration density can be achieved eventually.

(4) **Potentially low cost.** The cost-effective high quality and large area CVD graphene material can be made available with the rapid improvement of synthetic technology and transfer process. The simplicity of the GPD structure results in low-cost fabrication processes. The total cost of a single monolithic optoelectronic integrated optical receiver can be significantly reduced due to the small size and mass production as traditional IC chips from a 12-inch wafer. Moreover, as the GPD-based optical receivers can serve all optical communication systems, the demand would increase quickly as optical interconnects become significant in our daily life (such as "fiber to home" and "5G"). Therefore, this optical receiver can be cost-friendly compared with the commercial heterogeneous integrated optical receivers.

4 Conclusion

In conclusion, we have developed a CMOS backend process compatible method for integrating GPDs onto silicon CMOS ICs for the purpose of achieving a broadband optical receiver. The photocurrent signal amplifier ICs were obtained via a commercial silicon CMOS technology and GPDs were fabricated on the surface of the passivation layer of the IC chips via a micro-fabrication process. The monolithic OEIC-based broadband optical receivers could work at 500 kHz. With high-quality single crystal graphene and optimized fabrication process, the GPD-based optical receivers operating at tens of GHz can be available easily benefiting from potential high carrier mobility of graphene material. This work not only demonstrates a successful monolithic OEIC-based broadband optical receiver but also presents a feasible method for the monolithic integration of graphene optoelectronic devices and traditional silicon ICs.

Acknowledgments: This work was supported by the National Key Research and Development Program of China (Grant No. 2016YFB0402505, 2016YFA0202201), the National Basic Research Program of China (Grant No. 2015CB352100, 2013CB329205), the Natural Science Foundation of China (Grant Nos. 61675191, 61178051, 61335010, 61321063, 11404239, 61275169, 61227807, 61575108, 61504093), and the Opened Fund of the State Key Laboratory on Integrated Optoelectronics (No. IOSKL2015KF07, IOSKL2014KF15). We would like to acknowledge Assistant Professor Hongmei Chen from the Chinese Academy of Sciences for her support in revising.

References

- [1] Uemura H, Kurita Y, Furuyama H. 12.5 Gb/s optical driver and receiver ICs with double-threshold AGC for SATA out-of-band transmission. IEEE J Solid-State Circuits 2016;51:1-10.
- [2] Joo J, Jang K-S, Kim SH, et al. Silicon photonic receiver and transmitter operating up to 36 Gb/s for $\lambda \sim 1550$ nm. Opt Express 2015;23:12232-43.
- Chen YM, Wang ZG, Fan XN, Wang H, Li W. A 38 Gb/s to 43 Gb/s [3] monolithic optical receiver in 65 nm CMOS technology. IEEE Trans Circuits Syst I Reg Papers 2013;60:3173-81.
- [4] Pan Q, Hou ZX, Li Y, Poon AW, Yue CP. A 0.5-V p-well/deep n-well photodetector in 65-nm CMOS for monolithic 850-nm optical receivers. IEEE Photon Technol Lett 2014;26:1184-7.
- [5] Assefa S, Xia FN, Green WMJ, Schow CL, Rylyakov AV, Vlasov YA. CMOS-integrated optical receivers for on-chip interconnects. IEEE | Sel Topics Quant Electron 2010;16:1376-85.
- [6] Youn JS, Lee MJ, Park KY, Kim WS, Choi WY. Low-power 850 nm optoelectronic integrated circuit receiver fabricated in 65 nm complementary metal-oxide semiconductor technology. IET Circuits Devices Syst 2015;9:221-6.
- [7] Ang KW, Liow TY, Yu MB, et al. Low thermal budget monolithic integration of evanescent-coupled Ge-on-SOI photodetector on Si CMOS platform. IEEE J Sel Topics Quant Electron 2010;6:106-13.
- [8] Chaisakul P, Marris-Morini D, Frigerio J, et al. Integrated germanium optical interconnects on silicon substrates. Nat Phot 2014;8:482-8.
- [9] Sun C, Wade MT, Lee Y, et al. Single-chip microprocessor that communicates directly using light. Nature 2015;528:534-8.
- McComber KA, Duan XM, Liu JF, Michel J, Kimerling LC. Singlecrystal germanium growth on amorphous silicon. Adv Funct Mater 2012;22:1049-57.
- Droz NS, Lipson M. Scalable 3D dense integration of photonics [11] on bulk silicon. Opt Express 2011;19:17758-65.
- Zhang Z, Huang BJ, Zhang X, et al. Monolithic integration of Si₃N₄ microring filters with bulk CMOS IC through post-backend process. IEEE Photon Technol Lett 2015;27:1543-6.
- [13] Novoselov KS, Geim AK, Morozov SV, et al. Electric field effect in atomically thin carbon films. Science 2004;306:666-9.
- [14] Schwierz F. Graphene transistors. Nat Nanotechol 2010;5:487-96.
- [15] Han SJ, Garcia AV, Oida S, Jenkins KA, Haensch W. Graphene radio frequency receiver integrated circuit. Nat Commun 2014;5:3086-91.

- [16] Yeh C-H, Lain Y-W, Chiu Y-C, et al. Gigahertz flexible graphene transistors for microwave integrated circuits. ACS Nano 2014;8:7663-70.
- [17] Tao LQ, Wang DY, Song J, et al. Fabrication techniques and applications of flexible graphene-based electronic devices. J Semicond 2016;37:040001.
- [18] Bao QL, Zhang H, Wang B, et al. Broadband graphene polarizer. Nat Photon 2011;5:411-5.
- [19] Lim G-K, Chen Z-L, Clark J, et al. Giant broadband nonlinear optical absorption response in dispersed graphene single sheets. Nat Photon 2011;5:554-60.
- [20] Liu M, Yin XB, Ulin-Avila E, et al. A graphene-based broadband optical modulator. Nature 2011;474:64-7.
- [21] Xia FN, Mueller T, Lin YM, Garcia AV, Avouris P. Ultrafast graphene photodetector. Nat Nanotechnol 2009;4:839-43.
- [22] Mueller T, Xia FN, Avouris P. Graphene photodetectors for high-speed optical communications. Nat Photon 2010;4:297-301.
- [23] Gan XT, Shiue R-J, Gao YD, et al. Chip-integrated ultrafast graphene photodetector with high responsivity. Nat Photonics
- [24] Shiue R-J, Gao YD, Wang YF, et al. High-responsivity grapheneboron nitride photodetector and autocorrelator in a silicon photonic integrated circuit. Nano Lett 2015;15:7288-93.
- [25] Mak KF, Ju L, Wang F, Heinz TF. Optical spectroscopy of graphene: from the far infrared to the ultraviolet. Solid State Commun 2012;152:1341-9.
- [26] Schuler S, Schall D, Neumaier D, et al. Controlled generation of a p-n junction in a waveguide integrated graphene photodetector. Nano Lett 2016;16:7107-12.
- [27] Urich A, Unterrainer K, Mueller T. Intrinsic response time of graphene photodetectors. Nano Lett 2011;11:2804-8.
- [28] Sun D, Aivazian G, Jones AM, et al. Ultrafast hot-carrierdominated photocurrent in graphene. Nat Nanotechnol 2012;7:114-8.
- [29] Bolotin KI, Sikes KJ, Jiang Z, et al. Ultrahigh electron mobility in suspended graphene. Sol State Commun 2008;146:351-5.
- [30] Ito H, Furuta T, Kodama S, Ishibashi T. InP/InGaAs uni-travelling-carrier photodiode with 310 GHz bandwidth. Elect Lett 2000;36:1809-10.
- [31] Zhang YZ, Liu T, Meng B, et al. Broadband high photoresponse from pure monolayer graphene photodetector. Nat Commun 2013;4:1801-11.

- [32] Bae S, Kim H, Lee Y, et al. Roll-to-roll production of 30-inch graphene films for transparent electrodes. Nat Nanotechnol 2010;5:574-8.
- [33] Goossens S, Navickaite G, Monasterio C, et al. Broadband image sensor array based on graphene-CMOS integration. Nat Photon 2017;11:366-71.
- [34] Novoselov KS, Geim AK, Morozov SV, et al. Two-dimensional gas of massless dirac fermions in graphene. Nature 2005:438:197-200.
- [35] Nair RR, Blake P, Grigorenko AN, et al. Fine structure constant defines visual transparency of graphene. Science 2008;320:1308.
- [36] Furchi M, Urich A, Pospischil A, et al. Microcavity-integrated graphene photodetector. Nano Lett 2012;12: 2773-7.
- [37] Echtermeyer TJ, Britnell L, Jasnos PK, et al. Strong plasmonic enhancement of photovoltage in graphene. Nat Commun 2011:2:455-8.
- [38] Fang ZY, Liu Z, Wang YM, Ajayan PM, Nordlander P, Halas NJ. Graphene-antenna sandwich photodetector. Nano Lett 2012;12:3808-13.
- [39] Goykhman I, Sassi U, Desiatov B, et al. On-chip integrated silicon - graphene plasmonic Schottky photodetector with high responsivity and avalanche photogain. Nano Lett 2016;16:3005-13.
- [40] Pospischil A, Humer M, Furchi MM, et al. CMOS-compatible graphene photodetector covering all optical communication bands. Nat Photonics 2013;7:892-6.
- [41] Schall D, Neumaier D, Mohsin M, et al. 50 GBit/s photodetectors based on wafer-scale graphene for integrated silicon photonic communication systems. ACS Photon 2014;1:781-4.
- [42] Konstantatos G, Badioli M, Gaudreau L, et al. Hybrid graphene quantum dot phototransistors with ultrahigh gain. Nat Nanotechnol 2012;7:363-8.
- [43] Jiao LY, Zhang L, Wang XR, Diankov G, Dai HJ. Narrow graphene nanoribbons from carbon nanotubes. Nature 2009:458:877-80.
- [44] Brida D, Tomadin A, Manzoni C, et al. Ultrafast collinear scattering and carrier multiplication in graphene. Nat Commun 2013;4:1979-87.
- [45] Wu Y, Zou XM, Sun ML, et al. 200 GHz maximum oscillation frequency in CVD graphene radio frequency transistors. ACS Appl Mater Interface 2016;8:25645-9.